Simultaneous Measurement of Film Surface Topography and Thickness Variation using White-Light Interferometry

Katsuichi KITAGAWA*
Toray Engineering Co., Ltd.
1-1-45 Oe, Otsu, Shiga 520-2141, JAPAN

ABSTRACT

In vertical scanning white-light interferometry, two peaks appear in the interference waveform if a transparent film exists on the surface to be measured. We have developed an algorithm that is able to detect the position of these peaks quickly and accurately, and have put into practical use a film profiler that is able to simultaneously measure the profiles of both the front and back surfaces and the thickness distribution of a transparent film. This technique is applicable to transparent films with an optical thickness of approximately 1 μm or greater, and it is used effectively in the semiconductor and LCD manufacturing processes.

Keywords: interferometry, white light, surface profiler, transparent film, thickness, peak separation

1. INTRODUCTION

The technique of surface profile measurement using optical interference is widely used in industry as a non-contact and non-destructive method of quickly and accurately measuring the profile of microscopic surfaces. However, it is unable to provide an exact surface profile if the surface to be measured is covered with a transparent film due to the interference of beams originating from the back surface of the film.

This paper introduces the results of a study on a signal-processing algorithm used to measure the profile of surfaces covered with a transparent film by means of white-light interferometry (also called vertical scanning interferometry). We also describe here a non-contact film profiler, SP-500F, which incorporates the algorithm.

2. PRINCIPLES OF MEASUREMENT

The optical section of the equipment is shown in Figure 1.

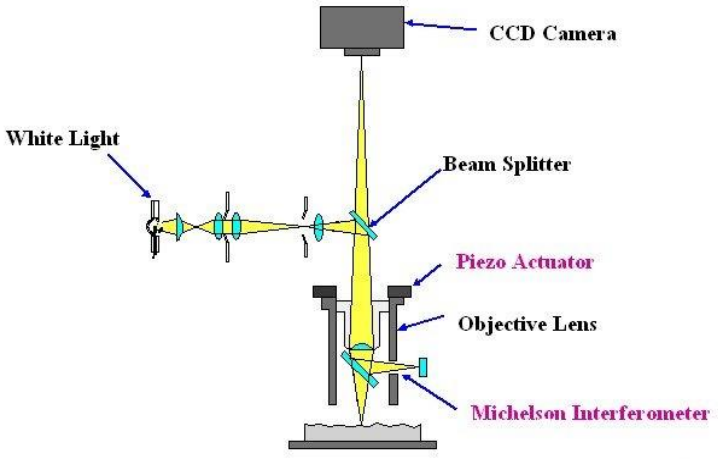

Figure 1. Schematic of an interference microscope.

* katsuichi_kitagawa@toray-eng.co.jp; http://www.scn.tv/corp/torayins/

The equipment uses white light with a short coherent length as the light source, and when it performs a vertical scan along the Z-axis of the interference microscope, the intensity signal of one charge-coupled device (CCD) pixel changes as shown in Figure 2, maximizing the modulation of the interference fringe at the point where the difference in the path length between the measurement light path and the reference light path becomes zero. By determining the Z-axis height that corresponds to the largest interference fringe modulation at every point in the TV camera, this technique measures en bloc the 3-dimensional profile in the field-of-view (FOV) of the camera.

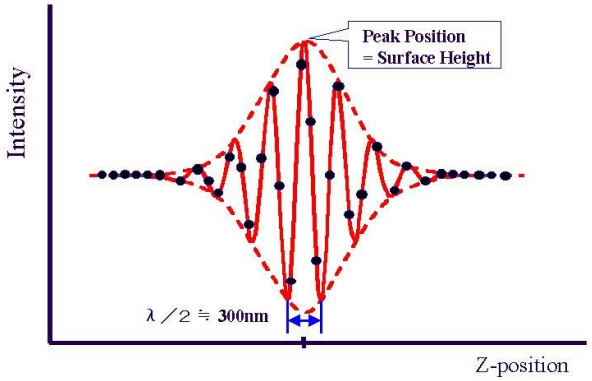

Figure 2. An example of a white-light interferogram. The black dots show sampled values, and the dotted line denotes the envelope.

Various methods have been proposed for the algorithm to detect the peak position of modulation, including the smoothing method,[1] the Hilbert transform method,[2] the Fourier transform method,[3] the centroid (center of gravity) method,[4] and the signal restoration method,[5] most of which assume that the peak is single. Therefore, if a film-covered surface is measured, superposition occurs between the reflected beams from the front surface and the reflected beams from the back surface, hampering correct measurement of the surface profile.

It has long been known that, if the thickness of a transparent film is greater than the coherent length, two peaks of reflection corresponding to the front and back surfaces appear on the interferogram, allowing simultaneous measurement of film thickness and surface height variations from those peak positions.[6-10]

However, the methods reported to date either require visual determination of peak positions,[6,7] or use a complex calculation algorithm,[9,10] and no automatic measuring device was available in the market for practical use until our development of such a device in 2002.

3. DEVELOPMENT OF THE ALGORITHM AND EXPERIMENTAL RESULTS

3.1 Test data

Using the SP-500 Surface Profiler,[5,11] a transparent film was measured and an interferogram was created as shown in Figure 3. The measurement was conducted under the following conditions:

(1) Illumination: A halogen lamp was used as the light source because a shorter coherent length is better able to achieve separation of peaks. The coherent length was approximately 1 μm.

(2) Speed of Z-axis scanning: The speed was set at 2.4 μm/sec with a sampling interval of 0.08 μm. This interval broadly corresponded to a quarter of the period of the interferogram.

(3) Subject for measurement: An oxide film with a thickness (D) of approximately 1 μm formed on a Si wafer was measured. The optical thickness ($n \cdot D$) was about 1.5 μm because the refractive index (n) was about 1.5. Since the coherent length was approximately 1 μm, the value was considered to be near the lower limit of values that permit the separation of peaks. In addition, the semiconductor and LCD manufacturing processes use various kinds of transparent films with thicknesses of several μm, such as resist films and coating films, and therefore, it was appropriate for practical purposes to select films with thicknesses of several micrometers as the subject for measurement.

(4) Range of scanning: The range was set at 5 μm. Since the number of images was 5/0.08 = 63, the total scanning time was approximately 2 seconds when a standard camera of 30 fps was used.

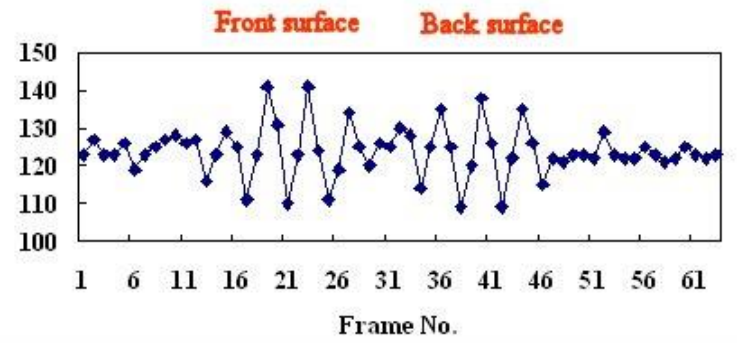

Figure 3. Interferogram used to test the proposed algorithm.

3.2 Calculation algorithm[12]

This algorithm, named KF (thicK Film), calculates the interference amplitudes from an interferogram. The results are interpreted as a histogram, and the automatic threshold selection method then finds the optimal threshold for peak separation. Finally, the peak position is determined for each of the separated peak regions.

3.2.1 Calculation procedure

(1) Step 1: Calculation of AC components

First determine the average value of the intensity data, and then calculate the AC components by subtracting the average value from each piece of data. The result is shown in Figure 4.

(2) Step 2: Calculation of amplitude

Square the AC components for the purpose of rectification. The result is shown in Figure 5.

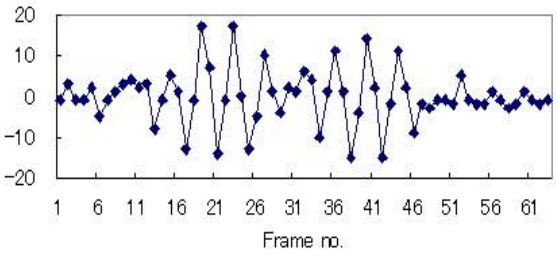

Figure 4. AC components of intensity signals.

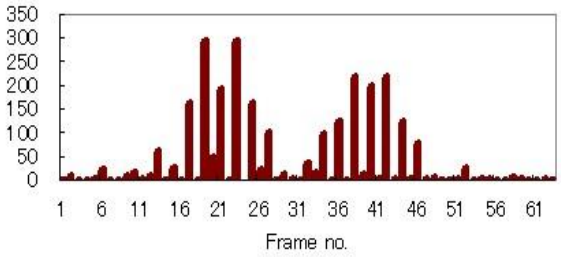

Figure 5. Squared values of AC components.

(3) Step 3: Separation of peaks

Taking the waveform data shown in Figure 5 as a histogram, determine the optimal threshold for peak separation, using Otsu's automatic threshold selection method in the field of processing to binary value imagery.[13]

More specifically, given a set of frequency values $n(i)$, (i = 1, L), where the number of observed value levels is L, and the observed value level is i, we take the intraclass variance, expressed by the following equation, as an objective function, and choose the threshold that minimizes the function:

$$f = \omega_1 \cdot \sigma_1^2 + \omega_2 \cdot \sigma_2^2, \quad (1)$$

where ω_1 and ω_2 are the frequencies of the classes, and σ_1^2 and σ_2^2 are the variances of the classes.

The values of the objective function are shown by the solid-line curve in Figure 6, with data number 30 being the threshold.

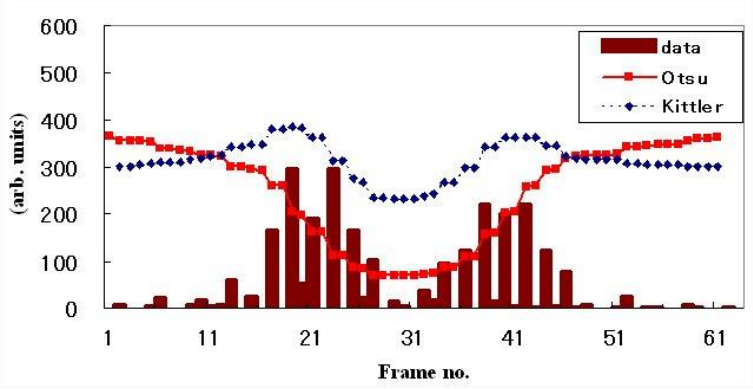

Figure 6. Two objective functions for threshold selection. The solid line denotes Otsu's method and the dotted line denotes Kittler's method.

(4) Step 4: Detection of peak position

Data number 30 separates the distribution into left and right peak regions. For each of the separated regions, the peak positions were detected by conventional methods. Here the waveform was smoothed, using the low-pass filter method, the most common method of peak position detection.[1] The calculation equation used for smoothing was the 19-point quadratic polynomial equation expressed by the following equation:

$$y(n) = (1/W)\ \Sigma w(i)\ \cdot x(n+i), \tag{2}$$

where i = 0, ±1, ±2, …, ±9; W, a normalizing coefficient, is the sum total of $w(i)$; $w(i)$ is the weighting factor, and the actual values are 269, 264, 249, 224, 189, 144, 89, 24, –51 and –136 starting from $w(0)$ for the 19-point method.

This calculation resulted in a smoothed curve (Figure 7), with two peak positions located at data numbers 21 and 40. Next, a quadratic curve was applied to three data points in the vicinity of the peaks in order to determine the interpolated peak positions, with the resolution being smaller than the sampling interval; this operation gave values of 21.17 and 39.61.

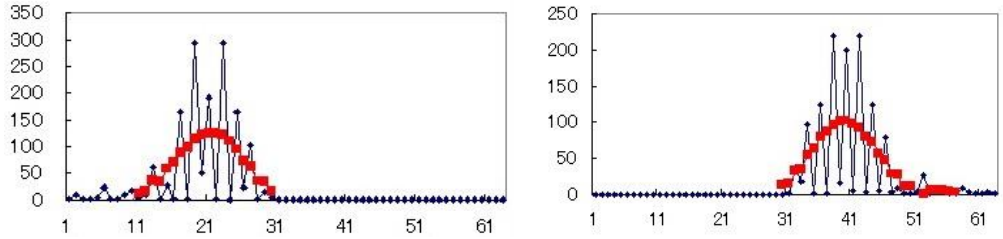

(a) Left peak (b) Right peak

Figure 7. Result of peak smoothing after peak separation.

(5) Step 5: Calculation of two surface heights and film thickness

Let the heights converted from the peak positions be z_{p1} and z_{p2}, and let the refractive index of the film be n; then:

i) the surface height of the transparent film = z_{p1};
ii) the film thickness $D = (z_{p1}-z_{p2})/n$; and
iii) the back-surface height of the film = $z_{p1}-D$.

This test, carried out with peak positions at 21.17 and 39.61, a sampling interval of 0.08 μm, and a film refractive index of n = 1.5, gave a surface height of 3.31 μm, a film thickness of 0.98 μm, and a back-surface height of 2.33 μm.

3.2.2 Comparison of peak separation algorithms

In addition to the above-mentioned Otsu's method, the method presented by Kittler et al.[14] provides another algorithm for automatic threshold selection based on the gray-level histogram.

The Kittler method takes the following equation as the objective function instead of Equation (1):

$$f = \omega_1 \cdot \log(\sigma_1/\omega_1) + \omega_2 \cdot \log(\sigma_2/\omega_2). \quad (3)$$

A comparison was made between these two methods for various cases. For the above experiment, no significant difference was found between the two methods, as shown in Figure 6. Figures 8(a) to 8(c) show other cases. The case of a greater difference between peak heights is shown in Figure 8(a), and the case of a smaller peak interval is shown in Figure 8(b). In both cases, Otsu's method gives more accurate results than Kittler's method, which is more effective when the variances of two peaks are very different from each other, as shown in Figure 8(c). With respect to the interference waveform, however, little difference is found normally in the variances. Given these results, Otsu's method was adopted for our purposes.

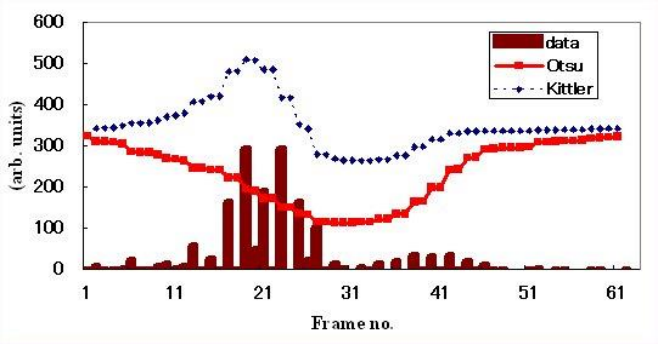

Figure 8(a). Two objective functions for threshold selection: The case of a greater difference between peak heights. The solid line denotes Otsu's method and the dotted line denotes Kittler's method.

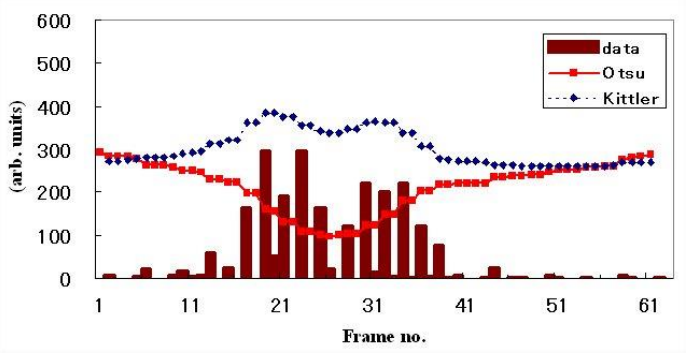

Figure 8(b). Two objective functions for threshold selection: The case of a smaller peak interval: The solid line denotes Otsu's method and the dotted line denotes Kittler's method.

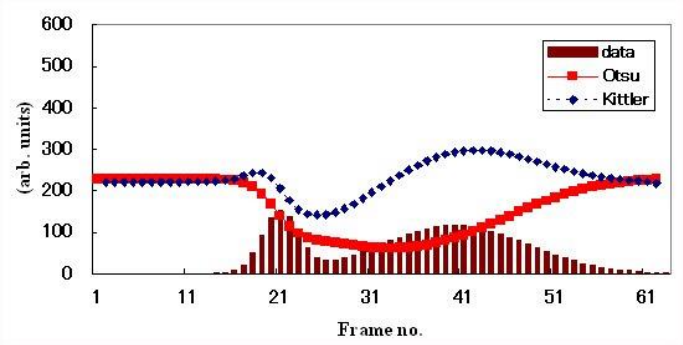

Figure 8(c). Two objective functions for threshold selection: The case of large difference in variance: The solid line denotes Otsu's method and the dotted line denotes Kittler's method.

3.3 Range of measurable film thickness

The KF method of measurement has a lower limit of measurable film thickness because it is based on the assumption that interferogram peaks can be separated. Oxide films with a thickness of 0.5-2 μm on a Si wafer were measured, and the minimum measurable thickness was found to be approximately 0.8 μm. Figure 9 shows two examples of interferograms.

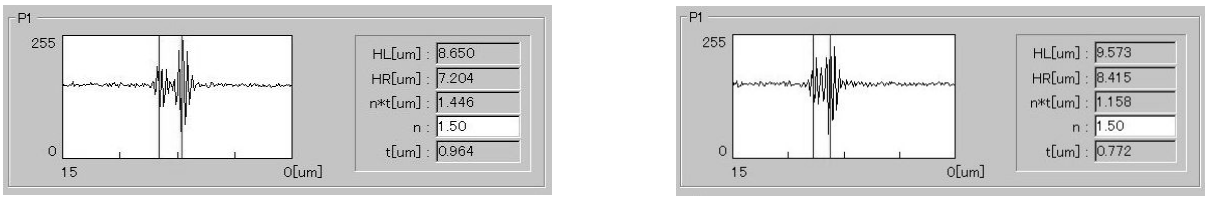

(a) Thickness = 0.96 μm (b) Thickness = 0.77 μm

Figure 9. Interferograms of oxide films on a Si wafer.

4. THE SP-500F FILM PROFILER

Software dealing with transparent films, based on the KF algorithm, was installed in the SP-500 Surface Profiler,[11] and the SP-500F Film Profiler, shown in Figure 10, was developed. Its major specifications are listed in Table 1.

Figure 10. SP-500F Film Profiler.

Table 1. Major specifications of the SP-500F Film Profiler.

Measurement Technique	Vertical Scanning Interferometry
Algorithm	KF Algorithm (Patent Pending)
Measurement Functions	Front Surface Profile, Back Surface Profile and Film Thickness Profile
Range of Measurement	0 to 100 μm (Optional: 0 to 350 μm)
Thickness Range	1 to 50 μm (optical thickness)
Objectives	Selectable from 2.5×, 5×, 10×, 20×, 50×
Measurement Speed	Dependent on the various parameters (typ. 10 sec)
Vertical Resolution	1 nm (Display Unit)
Thickness Measurement Repeatability	On the order of 0.1% (CV)
Measurement Array	Selectable from 512×480, 256×240, 128×120 (Optional: max. 1376×1040)
Computer System/OS	PC/Windows

5. EXAMPLES OF MEASUREMENTS

5.1. Step in film thickness

A step in oxide film formed on a Si wafer was measured, and the results are shown in 3-D representation in Figure 11. The measured surface step was 2.9 μm, and the film thickness was 4.0 μm in the higher area and 1.1 μm in the lower area. These thickness values agreed fully with measurements obtained by ellipsometry. It was also found that the back surface was correctly measured as a flat surface, with a supposed refractive index of 1.46.

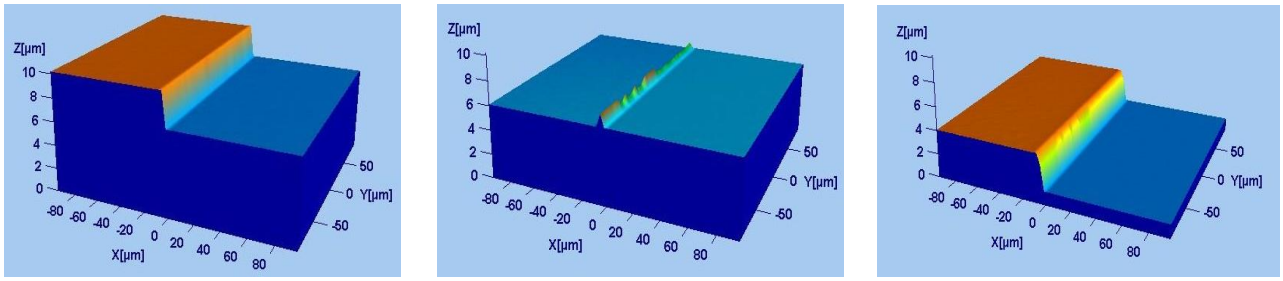

(a) Front surface (b) Back surface (c) Thickness

Figure 11. Measurement results of a SiO_2 film step on a Si wafer.

5.2 Tapered film

A tapered oxide film on a Si wafer was measured, and the results are shown in Figure 12. The conspicuously warped concave front and back surfaces and the tapered thickness profile of the film were measured.

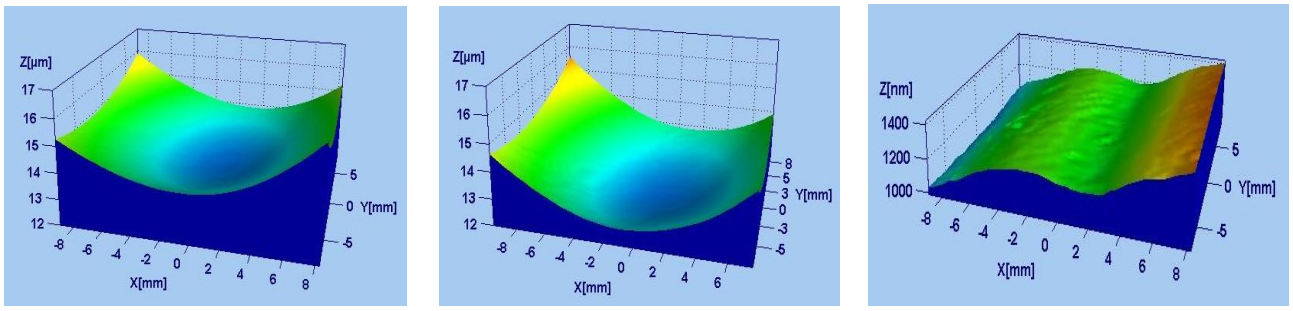

(a) Front surface (b) Back surface (c) Thickness

Figure 12. Measurement results of a tapered oxide film on a Si wafer.

5.3 LCD cell gap

The measurement results of the cell gap of an 8-segment liquid crystal display (LCD) are shown in Figure 13. A 20-mm FOV interferometer was used. The cell gap distribution of approximately 5 μm was measured en bloc through the thick glass plate.

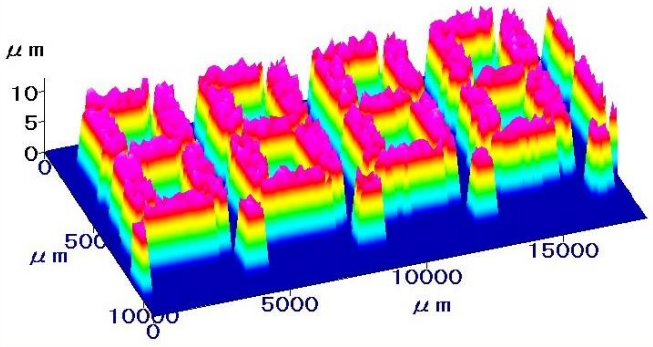

Figure 13. Measurement of cell gap.

5.4 Resist film with an unknown refractive index

The thickness distribution of a resist film on a glass plate was measured. Since the refractive index of the resist film was unknown, part of the film was peeled off, and the film profile was then measured. The surface step, which is equal to the physical thickness (D), was approximately 1.6 μm at the peeled portion, and the optical thickness ($n \cdot D$) was about 3.0 μm. These measurements allowed us to estimate the refractive index (n) at approximately 1.9.

The correctness of the refractive index can be justified by the fact that the plate surface of the peeled portion and the back surface of the film are flush on the same plane. The back surface profiles calculated with three different refractive indexes are shown in Figure 14. Visual estimation gives a result of $n = 1.90 \pm 0.02$.

The film thickness and back surface height were then recalculated with the obtained refractive index; the results are shown in Figure 15.

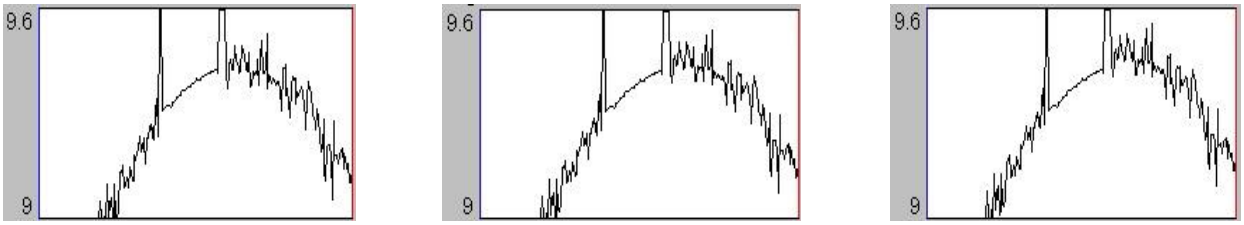

(a) n=1.88 (b) n=1.90 (c) n=1.92

Figure 14. Back surface profiles calculated with different refractive indexes (n). The peeled area is located at center left.

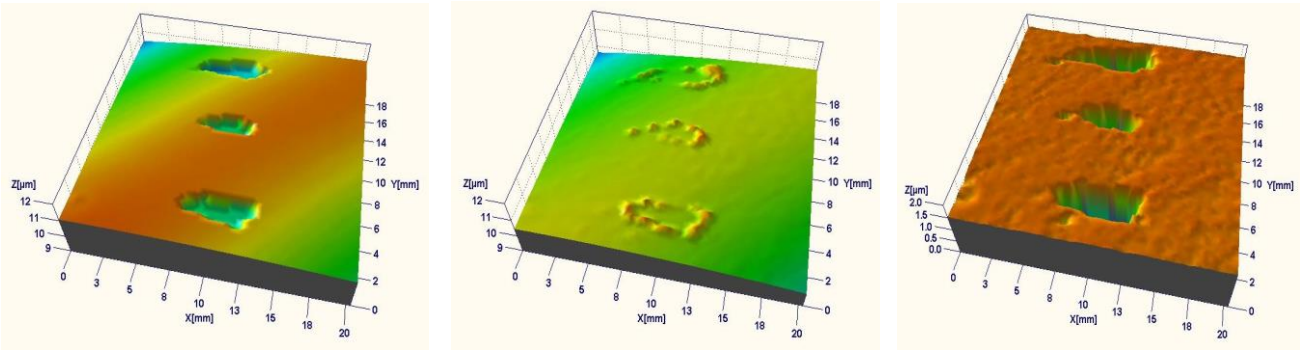

(a) Front surface (b) Back surface (c) Thickness

Figure 15. Measurement of resist film.

5.5 Water droplet surface

The profile of a water droplet on a glass plate was measured (Figure 16).

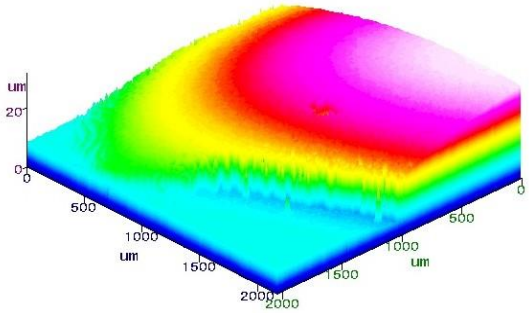

Figure 16. Measurement of a water droplet.

5.6 Repeatability of measurement

An oxide film on a Si wafer was measured repeatedly, giving the results shown in Figure 17. The measurement of film thickness produced the following data: mean value = 4.609 μm; standard deviation (σ) = 17 nm; and CV value = 0.36%.

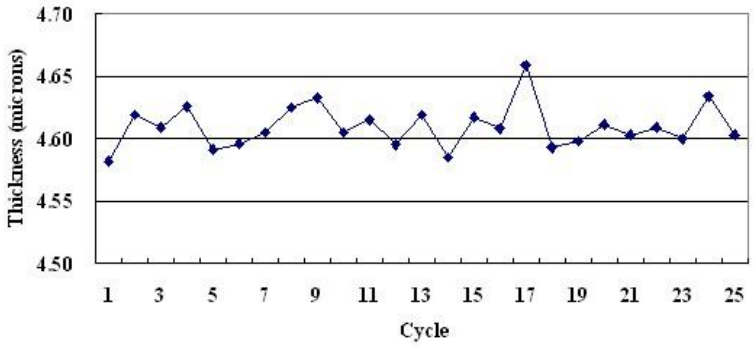

Figure 17. Repeatability of film thickness measurement.

In practical cases, the area-average thickness is often significant; therefore, on the resist film, averaging was performed in an area consisting of approximately 4000 pixels, which gave a mean value of 1.526 μm, a standard deviation (σ) of 3.4 nm and a CV value of 0.2%.

6. CONCLUSION

We developed an algorithm that is able to automatically detect the positions of two contrast peaks in an interferogram generated by vertical scanning white-light interferometry. Using this algorithm, we developed a non-contact Film Profiler, SP-500F, which allows simultaneous measurement of the front and back surface topography and the thickness variation of a transparent film.

The algorithm together with the film profiler make is possible to perform the following measurements, which are difficult to carry out under conventional methods:

(1) measurement of the profile of a surface covered with a transparent film; and
(2) 2-D measurement of film thickness distribution.

This system has already been introduced and used effectively in the semiconductor and LCD manufacturing processes.

ACKNOWLEDGEMENTS

The author would like to thank Professor Emeritus Hidemitsu Ogawa of the Tokyo Institute of Technology for valuable discussions.

REFERENCES

1. P.J. Caber, “Interferometric profiler for rough surface,” *Applied Optics* 32 (19), 3438-3441, 1993.
2. S.S.C. Chim and G.S. Kino, “Three-dimensional image realization in interference microscopy,” *Applied Optics* 31 (14), 2550-2553, 1992.
3. L. Deck and P. de Groot, “High-speed non-contact profiler based on scanning white light interferometry,” *Applied Optics* 33 (31), 7334-7338, 1994.
4. R. Dändliker, E. Zimmermann and G. Frosio, “Electronically scanned white-light interferometry: a novel noise-resistant signal processing,” *Optics Letters* 17 (9), 679-681, 1992.
5. A. Hirabayashi, H. Ogawa and K. Kitagawa, “Fast surface profiler by white-light interferometry by use of a new algorithm based on sampling theory,” *Applied Optics* 41 (23), 4876-4883, 2002.

6. P.A. Flournoy, R.W. McClure and G. Wyntjes, “White-light interferometric thickness gauge,” *Applied Optics* 11 (9), 1907-1915, 1972.
7. T. Tsuruta and Y. Ichihara, “Accurate measurement of lens thickness by using white-light fringes,” *Proc. ICO Conf. Opt. Methods in Sci. and Ind. Meas., Tokyo*, 369-372, 1974; *Japn. J. Appl. Phys., Suppl.* 14-1, 369-372, 1975.
8. B.S. Lee and T.C. Strand, “Profilometry with a coherence scanning microscope,” *Applied Optics* 29 (26), 3784-3788, 1990.
9. O. Nakamura and K. Toyoda, “Coherence probing of the patterns under films,” *Kougaku* 21 (7), 481-484, 1992 (in Japanese).
10. M. Itoh, R. Yamada, R. Tian, M. Tsai and T. Yatagai, “Broad-band light-wave correlation topography using wavelet transform,” *Optical Review* 2 (2), 135-138, 1995.
11. Toray Inspection Equipment Home Page, (Toray Engineering Co., 2006), http://www.scn.tv/corp/torayins/.
12. K. Kitagawa, “3-D profiler of a transparent film using white-light interferometry,” *Proc. of SICE Annual Conference 2004 in Sapporo*, 585-590, 2004.
13. N. Otsu, “An automatic threshold selection method based on discriminant and least squares criteria,” *Trans. of IECE* 63-D (4), 349-356, 1980 (in Japanese).
14. J. Kittler and J. Illingworth, “Minimum error thresholding,” *Pattern Recognition* 19 (1), 41-47, 1986.

This material is the final manuscript for:
[Invited Talk] K. Kitagawa, " Simultaneous Measurement of Film Surface Topography and Thickness Variation using White-Light Interferometry ", Optics East Symposium, #6375A-7 (2006.10.3 Boston).

Published in Proc. of SPIE Vol. 6375, 637507 (2006).